A Letters Journal Exploring the Frontiers of Physics

May 2010

EPL, **90** (2010) 38002
doi: 10.1209/0295-5075/90/38002

www.epljournal.org

On the dependence of the leak rate of seals on the skewness of the surface height probability distribution

B. Lorenz[1,2] and B. N. J. Persson[1(a)]

[1] *IFF, FZ Jülich - D-52425 Jülich, Germany, EU*
[2] *IFAS, RWTH Aachen University - D-52074 Aachen, Germany, EU*

received 11 March 2010; accepted in final form 26 April 2010
published online 25 May 2010

PACS 83.50.Lh – Slip boundary effects (interfacial and free surface flows)
PACS 46.55.+d – Tribology and mechanical contacts
PACS 68.35.Np – Adhesion

Abstract – Seals are extremely useful devices to prevent fluid leakage. We present experimental result which show that the leak rate of seals depend sensitively on the skewness in the height probability distribution. The experimental data are analyzed using the critical-junction theory. We show that using the top power spectrum results in good agreement between theory and experiment.

A seal is a device for closing a gap or making a joint fluid tight [1]. Seals play a crucial role in many modern engineering devices, and the failure of seals may result in catastrophic events, such as the Challenger disaster. In spite of its apparent simplicity, it is not easy to predict the leak rate and (for dynamic seals) the friction forces [2]. The main problem is the influence of surface roughness on the contact mechanics at the seal-substrate interface. Most surfaces of engineering interest have surface roughness on a wide range of length scales [3], *e.g.*, from cm to nm, which will influence the leak rate and friction of seals, and accounting for the whole range of surface roughness is impossible using standard numerical methods, such as the finite-element method.

Randomly rough surfaces have Gaussian height probability distribution but many surfaces of engineering interest have skewed distributions which may affect the leak rate of seals. To illustrate this we consider an extreme case: a rigid solid block with a flat surface in contact with a rigid substrate with periodic "roughness" as in fig. 1. The substrate surfaces in (a) and (b) have the same root-mean-square roughness and the same surface roughness power spectrum, but it is clear that in (a) the empty volume between the surfaces is larger than in (b), resulting in a larger leak rate. In the real situation the roughness is not periodic and the solids are not rigid, but one may expect a higher leak rate for the situation where the asymmetry of the height profile is as for case (a).

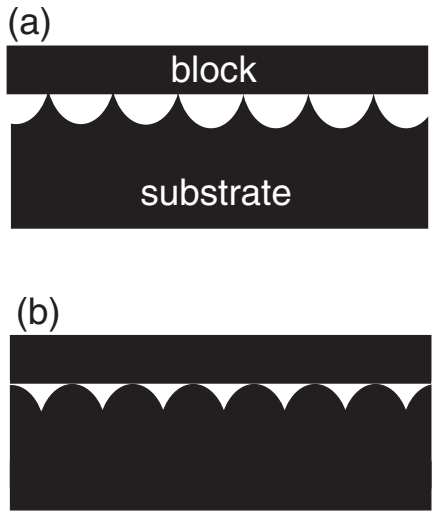

Fig. 1: Contact between a rigid block with a flat surface and a rigid substrate with periodic surface structures. The two substrate surfaces in (a) and (b) have the same surface roughness power spectrum. Note that the empty volume between the surfaces is much larger in case (a) than in case (b).

To study the point discussed above, we have performed experiments using sandpaper which has a skewed height probability distribution as in fig. 1(a). We have also used surfaces with "inverted" surface roughness profile by producing a "negative" of the sandpaper surface using silicon rubber. In the latter experiments we squeezed a silicon rubber ring, which was cross-linked with the sandpaper surface as the substrate, against a flat glass

(a) E-mail: b.persson@fz-juelich.de

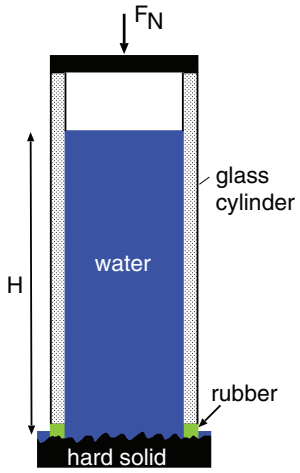

Fig. 2: (Colour on-line) Experimental set-up for measuring the leak rate of seals. A glass (or PMMA) cylinder with a rubber ring attached to one end is squeezed against a hard substrate with well-defined surface roughness. The cylinder is filled with water, and the leak rate of the water at the rubber-countersurface is detected by the change in the height of the water in the cylinder.

surface. By comparing the measured leak rate for this configuration with that for a silicon ring with flat bottom surface squeezed against the same sandpaper surface, we are able to address the problem illustrated in fig. 1.

We briefly describe the leak rate model [3–8] and the experimental set-up used in this study. Consider the fluid leakage through a rubber seal, from a high-pressure $P_{\rm a}$ fluid region, to a low-pressure $P_{\rm b}$ fluid region. In our experimental study we have used the experimental set-up shown in fig. 2 for measuring the leak rate of seals. A glass (or PMMA) cylinder with a rubber ring attached to one end is squeezed against a hard substrate with well-defined surface roughness. The cylinder is filled with water, and the leak rate of the water at the rubber-countersurface is detected by the change in the height of the water in the cylinder. Thus $P_{\rm a}-P_{\rm b}=\rho g H$, where H is the height of the water column, and ρ the mass density of water. For further experimental details, see refs. [4,7].

Assume that the nominal contact region between the rubber and the hard countersurface is rectangular with area $L_x\times L_y$, with $L_y>L_x$. We assume that the high-pressure fluid region is for $x<0$ and the low-pressure region for $x>L_x$. We "divide" the contact region into squares with the side $L_x=L$ and the area $A_0=L^2$ (this assumes that $N=L_y/L_x$ is an integer, but this restriction does not affect the final result). Now, let us study the contact between the two solids within one of the squares as we increase the magnification ζ. We define $\zeta=L/\lambda$, where λ is the resolution. We study how the apparent contact area (projected on the xy-plane), $A(\zeta)$, between the two solids depends on the magnification ζ. At the lowest magnification we cannot observe any surface roughness, and the contact between the solids appears to be complete *i.e.*, $A(1)=A_0$. As we increase the magnification we will observe some interfacial roughness, and the (apparent) contact area will decrease. At high enough magnification, say $\zeta=\zeta_{\rm c}$, a percolating path of non-contact area will be observed for the first time. We denote the most narrow constriction along this percolation path as the *critical constriction*. The critical constriction will have the lateral size $\lambda_{\rm c}=L/\zeta_{\rm c}$ and the surface separation at this point is denoted by $u_{\rm c}$. We can calculate $u_{\rm c}$ using a recently developed contact mechanics theory [9] (see below). As we continue to increase the magnification we will find more percolating channels between the surfaces, but these will have more narrow constrictions than the first channel which appears at $\zeta=\zeta_{\rm c}$, and as a first approximation one may neglect the contribution to the leak rate from these channels [6].

A first rough estimate of the leak rate is obtained by assuming that all the leakage occurs through the critical percolation channel, and that the whole pressure drop $\Delta P=P_{\rm a}-P_{\rm b}$ (where $P_{\rm a}$ and $P_{\rm b}$ is the pressure to the left and right of the seal) occurs over the critical constriction (of width and length $\lambda_{\rm c}\approx L/\zeta_{\rm c}$ and height $u_{\rm c}$). We refer to this theory as the *critical-junction* theory. If we approximate the critical constriction as a pore with rectangular cross-section (width and length $\lambda_{\rm c}$ and height $u_{\rm c}\ll\lambda_{\rm c}$), and if we assume an incompressible Newtonian fluid, the volume flow per unit time through the critical constriction will be given by (Poiseuille flow)

$$\dot{Q}=\frac{u_{\rm c}^3}{12\eta}\Delta P, \tag{1}$$

where η is the fluid viscosity. In deriving (1) we have assumed laminar flow and that $u_{\rm c}\ll\lambda_{\rm c}$, which is always satisfied in practice. Finally, since there are $N=L_y/L_x$ square areas in the rubber-countersurface (apparent) contact area, we get the total leak rate

$$\dot{Q}=\frac{L_y}{L_x}\frac{u_{\rm c}^3}{12\eta}\Delta P. \tag{2}$$

Note that a given percolation channel could have several narrow (critical or nearly critical) constrictions of nearly the same dimension which would reduce the flow along the channel. But in this case one would also expect more channels from the high- to the low-pressure fluid side of the junction, which would tend to increase the leak rate. These two effects will, at least in the simplest picture, compensate each other (see ref. [6]). The effective medium theory presented in ref. [7] includes (in an approximate way) all the flow channels, but gives results very similar to the critical-junction theory described above [10].

To complete the theory we must calculate the separation $u_{\rm c}$ of the surfaces at the critical constriction. We first determine the critical magnification $\zeta_{\rm c}$ by assuming that the apparent relative contact area at this point is given by percolation theory. Thus, the relative contact area $A(\zeta)/A_0\approx 1-p_{\rm c}$, where $p_{\rm c}$ is the so called percolation

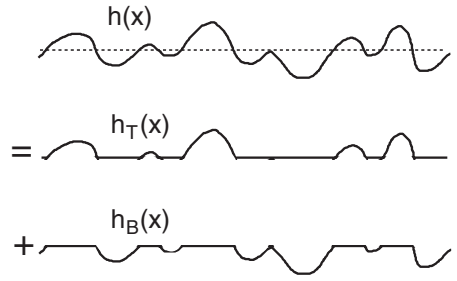

Fig. 3: The surface profile $h(x)$ is decomposed into a top $h_{\rm T}(x)$ and a bottom $h_{\rm B}(x)$ profile.

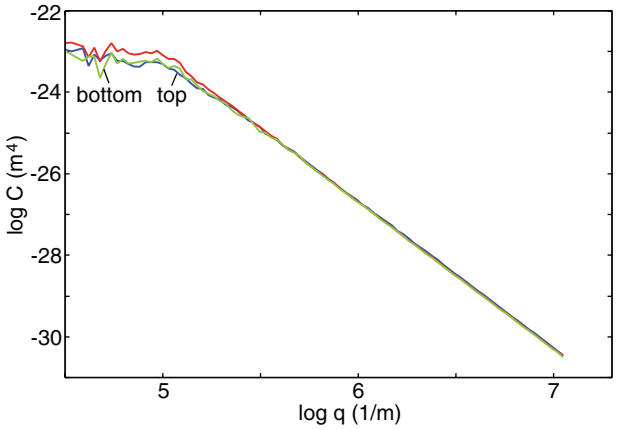

Fig. 4: (Colour on-line) The power spectrum $C(q)$ and the top $C^*_{\rm T}(q)$ and bottom $C^*_{\rm B}(q)$ power spectrum for a mathematically generated randomly rough surface with a Gaussian height probability distribution. The surface is self-affine fractal for $q > 10^5\,{\rm m}^{-1}$ with the fractal dimension $D_{\rm f} = 2.2$ and the root-mean-square roughness $0.8\,\mu$m.

threshold [11]. Numerical contact mechanics studies, such as those presented in ref. [6] and ref. [12], typically give $p_{\rm c}$ between 0.5 and 0.6. For finite-sized systems the percolation will, on the average, occur for (slightly) smaller values of $p_{\rm c}$, and fluctuations in the percolation threshold will occur between different realizations of the same physical system. Here we use $p_{\rm c} = 0.6$ to determine the critical magnification $\zeta = \zeta_{\rm c}$.

The (apparent) relative contact area $A(\zeta)/A_0$ and the interfacial separation $u_1(\zeta)$ at the magnification ζ can be obtained using the contact mechanics formalism developed elsewhere [9,13–19]. We define $u_1(\zeta)$ to be the (average) height separating the surfaces which appear to come into contact when the magnification decreases from ζ to $\zeta - \Delta\zeta$, where $\Delta\zeta$ is a small (infinitesimal) change in the magnification. Since the surfaces of the solids are everywhere rough the actual separation between the solid walls will fluctuate around the average $u_1(\zeta)$. Thus we expect $u_{\rm c} = \alpha u_1(\zeta_{\rm c})$, where $\alpha < 1$ (but of order unity). We note that α is due to the surface roughness which occur at length scales shorter than $\lambda_{\rm c}$, see ref. [7].

In the contact mechanics theory of Persson, the surface roughness enter only via the surface roughness power spectrum

$$C(q) = \frac{1}{(2\pi)^2}\int {\rm d}^2x\ \langle h(\mathbf{x})h(\mathbf{0})\rangle {\rm e}^{-i\mathbf{q}\cdot\mathbf{x}},$$

where $\langle \ldots \rangle$ stands for ensemble average, and where we have assumed $\langle h\rangle = 0$. A randomly rough surface has a Gaussian height probability distribution, $P(h)$, but many surfaces of practical use have a skewed height distribution. For this latter case it is useful to introduce the *top* and *bottom* power spectra defined as follows [3]:

$$C_{\rm T}(q) = \frac{1}{(2\pi)^2}\int {\rm d}^2x\ \langle h_{\rm T}(\mathbf{x})h_{\rm T}(\mathbf{0})\rangle {\rm e}^{-i\mathbf{q}\cdot\mathbf{x}},$$

$$C_{\rm B}(q) = \frac{1}{(2\pi)^2}\int {\rm d}^2x\ \langle h_{\rm B}(\mathbf{x})h_{\rm B}(\mathbf{0})\rangle {\rm e}^{-i\mathbf{q}\cdot\mathbf{x}},$$

where $h_{\rm T}(\mathbf{x}) = h(\mathbf{x})$ for $h > 0$ and zero otherwise, while $h_{\rm B}(\mathbf{x}) = h(\mathbf{x})$ for $h < 0$ and zero otherwise. These are "rectified" profiles; see fig. 3. It is clear by symmetry that for a randomly rough surface with Gaussian height distribution, $C_{\rm T}(q) = C_{\rm B}(q)$. If $n_{\rm T}$ and $n_{\rm B}$ are the fractions of the nominal surface area (*i.e.*, the surface area projected on the xy-plane) where $h > 0$ and $h < 0$, respectively, then we also define $C^*_{\rm T}(q) = C_{\rm T}(q)/n_{\rm T}$ and $C^*_{\rm B}(q) = C_{\rm B}(q)/n_{\rm B}$. Roughly speaking, $C^*_{\rm T}$ would be the power spectrum resulting if the actual bottom profile (for $h < 0$) was replaced by a mirrored top profile (for $h > 0$). A similar statement holds for $C^*_{\rm B}$. For randomly rough surfaces with Gaussian height distribution we expect $C^*_{\rm T}(q) = C^*_{\rm B}(q) \approx C(q)$. That this is indeed the case is illustrated in fig. 4 which shows the calculated $C(q)$, $C^*_{\rm T}(q)$ and $C^*_{\rm B}(q)$ for a mathematically generated randomly rough surface with a Gaussian height probability distribution. The surface is self-affine fractal for $q > 10^5\,{\rm m}^{-1}$ with the fractal dimension $D_{\rm f} = 2.2$ and the root-mean-square roughness $0.8\,\mu$m.

The contact mechanics theory of Persson can be applied approximately to surfaces with skewed height distribution. However in this case, at least for small squeezing pressures, one should use $C^*_{\rm T}(q)$ rather than $C(q)$ in order to better represent the surface roughness. We will show below that by using $C^*_{\rm T}(q)$ we can quantitatively understand the leak rate of rubber seals squeezed against surfaces with skewed height probability distribution. We note that for small squeezing pressures the rubber will only probe the upper part of the substrate surface roughness profile. Hence it is clear that the dependence of the area of contact on the magnification, which determines the critical magnification where the non-contact area percolate, will be more accurately described using the top power spectrum. Referring to fig. 1 it is also clear that the largest volume of fluid between the surfaces will occur above the average surface plane, at least for small squeezing pressures. Finally we note that using the top

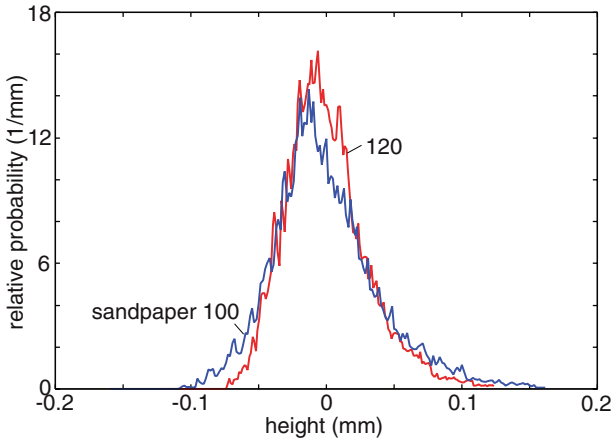

Fig. 5: (Colour on-line) The surface height probability distribution for sandpaper 100 and 120 surfaces with the root-mean-square roughness amplitudes 40 μm and 31 μm. The two surfaces have the skewness $\langle h^3\rangle/\langle h^2\rangle^{3/2} = 0.85$ and 0.82, respectively.

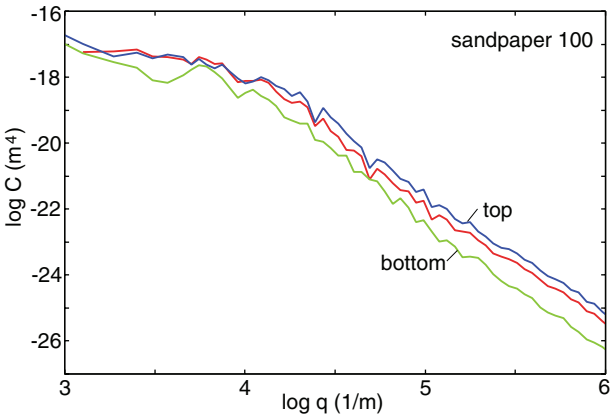

Fig. 6: (Colour on-line) Surface roughness power spectrum of sandpaper 100 surface. The three curves are the surface roughness power spectrum $C(q)$ of the original surface (red), and the top $C_{\rm T}^*(q)$ (blue) and bottom $C_{\rm B}^*(q)$ (green) surface roughness power spectrum. The surface has the root-mean-square roughness 40 μm. The fraction of the (projected) surface area above the average plane is about 0.44.

power spectrum does not mean that we do not account for the surface roughness below the average plane, but rather the region below the average plane is assumed to be replaced by a mirrored top profile.

We have performed experiments using two sandpaper surfaces (corundum paper, grit size 100 and 120) with the the root-mean-square roughness 40 μm and 31 μm. From the measured surface topography we obtain the height probability distribution $P(h)$ (fig. 5) and the surface roughness power spectrum shown in figs. 6 and 7, respectively. Note that for both surfaces $P(h)$ is asymmetric with a tail towards higher h. This is easy to understand: sandpaper surfaces consist of particles with sharp edges pointing above the surface, while the region between the

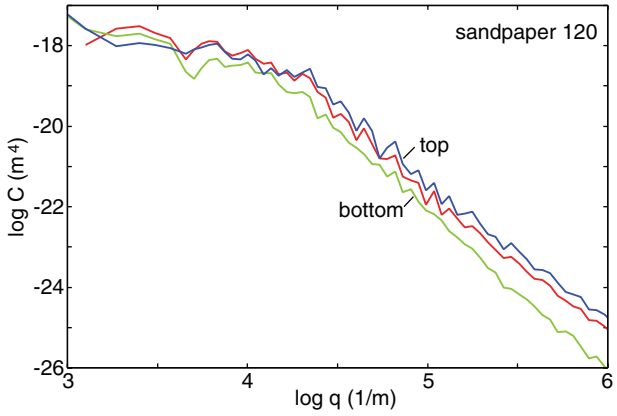

Fig. 7: (Colour on-line) Surface roughness power spectrum of sandpaper 120 surface. The three curves are the surface roughness power spectrum $C(q)$ of the original surface (red), and the top $C_{\rm T}^*(q)$ (blue) and bottom $C_{\rm B}^*(q)$ (green) surface roughness power spectrum. The surface has the root-mean-square roughness 31 μm. The fraction of the (projected) surface area above the average plane is about 0.45.

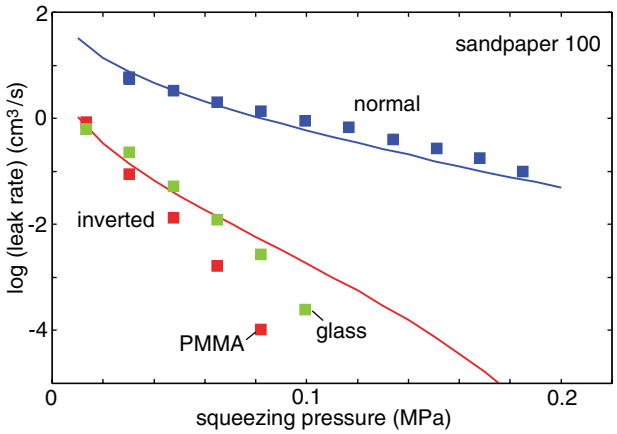

Fig. 8: (Colour on-line) Square symbols: the measured leak rate for sandpaper 100 substrate (upper symbols) and for an inverted surface (lower symbols). The solid lines are the calculated leak rate using the critical-junction theory with the percolation threshold $p_{\rm c} = 0.6$. In the calculation for the top curve we used the top power spectrum $C_{\rm T}^*(q)$ obtained from the measured surface topography. For the inverted surface (bottom curve) we used the bottom power spectrum $C_{\rm B}^*(q)$. The measured rubber elastic modulus $E = 2.3$ MPa and the fluid pressure difference $\Delta P = P_{\rm a} - P_{\rm b} = 10$ kPa obtained from the height of the water column. In the calculations we have used $\alpha = 1$ (upper curve) and $\alpha = 0.8$ (lower curve).

particles is filled with a resin-binder making the valleys smoother and wider than the peaks (as in fig. 1(a)), which result in an asymmetric $P(h)$ as observed.

In fig. 8 we show the measured leak rate for sandpaper 100 substrate (upper squares) and for an inverted surface (lower squares). The solid lines are the calculated leak rate using the critical-junction theory. In the calculation for the top curve we used the top power spectrum $C_{\rm T}^*(q)$

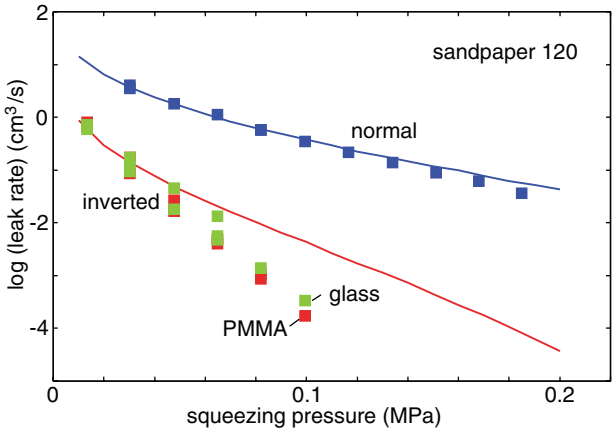

Fig. 9: (Colour on-line) Square symbols: the measured leak rate for sandpaper 120 substrate (upper symbols) and for an inverted surface (lower symbols). The solid lines are the calculated leak rate using the critical-junction theory with the percolation threshold $p_c = 0.6$. In the calculation for the top curve we used the top power spectrum $C_T^*(q)$ obtained from the measured surface topography. For the inverted surface (bottom curve) we used the bottom power spectrum $C_B^*(q)$. The measured rubber elastic modulus $E = 2.3\,\mathrm{MPa}$ and the fluid pressure difference $\Delta P = P_a - P_b = 10\,\mathrm{kPa}$ obtained from the height of the water column. In the calculations we have used $\alpha = 1$ (upper curve) and $\alpha = 0.8$ (lower curve).

obtained from the measured surface topography. For the inverted surface (bottom curve) we used the bottom power spectrum $C_B^*(q)$ of the sandpaper surface.

In fig. 9 we show similar results for the sandpaper 120 substrate (upper symbols) and for an inverted surface (lower symbols). Note in figs. 8 and 9 the huge difference (roughly two orders of magnitude) between the leak rate for the two different configurations, involving the original and inverted surface topographies. Note that the theory is able to describe the observed effect if the top power spectrum is used in the analysis (which means using the bottom power spectrum of the sandpaper surfaces in the case of the inverted surfaces). However, for the case of the inverted surfaces the leak rate for large enough squeezing pressure decreases faster with the squeezing pressure than is predicted by the theory. We attribute this to the influence of adhesion on the leak rate. That is, the asperities of the inverted surface are quite smooth (they arise from the relative smooth polymer (resin) film in the valleys between the particles of the original sand paper surfaces) which allow for effective adhesion between the rubber and the glass and PMMA surfaces[1]. We note here that the glass surfaces were not cleaned chemically and therefore probably covered by nanometer thick organic contamination layers[2]. Thus one expect a dewetting transition [20,21] in the asperity contact regions between the substrate surface and the silicon rubber surface, resulting in an effective adhesion which pulls the surfaces in closer contact than expected by just the influence of the squeezing pressure. Preliminary calculations including adhesion indeed support this picture and will be reported on elsewhere.

To summarize, we have compared experimental data with theory for the leak rate of seals. The theory is based on percolation theory and a recently developed contact mechanics theory. The experiments are for a) silicon rubber with a smooth surface in contact with two sandpaper surfaces, and b) for silicon rubber surfaces prepared by cross-linking the rubber in contact with the sandpaper surfaces, and then squeezing the rough rubber surfaces against flat glass and PMMA surfaces. The elastic properties of the rubber and the surface topography of the sandpaper and PMMA surfaces are fully characterized. We have shown that using the top power spectrum in the theory results in good agreement between theory and experiment.

* * *

We thank M. Chaudhury for useful communication about the work of adhesion (see footnotes [1] and [2]). This work, as part of the European Science Foundation EUROCORES Program FANAS, was supported from funds by the DFG and the EC Sixth Framework Program, under contract No. ERAS-CT-2003-980409.

REFERENCES

[1] Flitney R., *Seals and Sealing Handbook* (Elsevier) 2007.
[2] Mofidi M., Prakash B., Persson B. N. J. and Albohr O., *J. Phys.: Condens. Matter*, **20** (2008) 085223.
[3] See, *e.g.*, Persson B. N. J., Albohr O., Tartaglino U., Volokitin A. I. and Tosatti E., *J. Phys.: Condens. Matter*, **17** (2005) R1.
[4] Lorenz B. and Persson B. N. J., *EPL*, **86** (2009) 44006.
[5] Persson B. N. J., Albohr O., Creton C. and Peveri V., *J. Chem. Phys.*, **120** (2004) 8779.
[6] Persson B. N. J. and Yang C., *J. Phys.: Condens. Matter*, **20** (2008) 315011.
[7] Lorenz B. and Persson B. N. J., *Eur. Phys. J. E*, **31** (2010) 159.
[8] Carbone G. and Bottiglione F., *J. Mech. Phys. Solids*, **56** (2008) 2555.

[1] The work of adhesion $w = \gamma_1 + \gamma_2 - \gamma_{12}$ between PDMS and Plexiglas (PMMA) in water has not been measured but can be estimated to be about $55\,\mathrm{mJ/m^2}$.

[2] If the glass is clean, water wets it almost completely, and the work of adhesion between glass and PDMS through water may be zero or even slightly negative, *i.e.* there may be a repulsion instead of attraction. However, in general, organic contamination is strongly adsorbed to glass: the organic molecules that float in air and adsorbs to surface like glass are oxidized and interact with the surface by some strong specific interaction. They are not easy to remove by water. In this case one may estimate the work of adhesion by $w \approx (1-\phi) \times w(\mathrm{glass|water|PDMS}) + \phi \times w(\mathrm{hydrocarbon|water|PDMS})$, where ϕ is the fraction of the surface occupied by organic contamination. Typically, one expect $w(\mathrm{glass|water|PDMS}) \approx 0$ and $w(\mathrm{hydrocarbon|water|PDMS}) \approx 80\,\mathrm{mJ/m^2}$.

[9] Yang C. and Persson B. N. J., *J. Phys.: Condens. Matter*, **20** (2008) 215214.
[10] An alternative to using the effective medium approach to calculate the leak rate of seals, one may use the so-called critical path analysis. This approach has recently been applied to seals (Bottiglione F., Carbone G., Mangialardi L. and Mantriota G., *J. Appl. Phys.*, **106** (2009) 104902) but in contrast to the effective medium theory, there enters two parameters which are not easy to obtain from theory.
[11] Stauffer D. and Aharony A., *An Introduction to Percolation Theory* (CRC Press) 1991.
[12] See paper F in Sahlin F., *Lubrication, contact mechanics and leakage between rough surfaces*, PhD Thesis, 2008.
[13] Persson B. N. J., *J. Chem. Phys.*, **115** (2001) 3840.
[14] Persson B. N. J., *Phys. Rev. Lett.*, **99** (2007) 125502.
[15] Persson B. N. J., *Surf. Sci. Rep.*, **61** (2006) 201.
[16] Persson B. N. J., *Eur. Phys. J. E*, **8** (2002) 385.
[17] Persson B. N. J., Bucher F. and Chiaia B., *Phys. Rev. B*, **65** (2002) 184106.
[18] Lorenz B. and Persson B. N. J., *J. Phys.: Condens. Matter*, **201** (2009) 015003.
[19] Persson B. N. J., *J. Phys.: Condens. Matter*, **20** (2008) 312001.
[20] Persson B. N. J., Volokitin A. and Tosatti E., *Eur. Phys. J. E*, **11** (2003) 409.
[21] Martin A., Rossier O., Buguin A., Auroy P. and Brochard-Wyart F., *Eur. Phys. J. E*, **3** (2000) 337.